Dimension-Reduced Rx Beamforming Optimized for Simultaneous Detection and Estimation

NADAV NEUBERGER, Member, IEEE
Fraunhofer Institute for High Frequency Physics and Radar Techniques Wachtberg, Germany

RISTO VEHMAS
Elettronica GmbH Meckenheim, Germany

JOACHIM H. G. ENDER, Fellow, IEEE
Fraunhofer Institute for High Frequency Physics and Radar Techniques Wachtberg, Germany

Phased array radar systems are indispensable in many applications requiring robust sensing of the environment. To achieve sensitive target detection and accurate direction-of-arrival (DOA) estimation, a large number of receiving antenna elements are needed. The high dimension of the element-level data inevitably leads to a large computational burden for digital signal processing. This problem can be overcome by transforming the element-level data into a lower dimensional beamspace. In this article, we present a novel parameter-controlled design method to construct this transformation. If the dimension reduction is not too drastic, it jointly achieves optimal detection and DOA estimation performance. Otherwise, it meets predefined performance criteria by exploiting an acceptable tradeoff between detection and DOA estimation performance. We propose a general design tool, which is not limited to a specific array configuration. It comprises a precalculated set of plots, providing the radar designer an overview of possible performance for a given scenario. We describe a straightforward method to construct the corresponding transformation. Numerical studies highlight the superiority of the proposed design method.

Manuscript received July 6, 2020; revised November 18, 2020; released for publication January 26, 2021. Date of publication February 22, 2021; date of current version August 9, 2021.

DOI. No. 10.1109/TAES.2021.3060758

Refereeing of this contribution was handled by R. Adve.

Authors' addresses: Nadav Neuberger and Joachim H. G. Ender are with the Department of Array-Based Radar Imaging, Fraunhofer Institute for High Frequency Physics and Radar Techniques FHR, 53343 Wachtberg, Germany, E-mail: (nadav.neuberger@fhr.fraunhofer.de; joachim.ender@fhr.fraunhofer.de); Risto Vehmas is with Elettronica GmbH, 53340 Meckenheim, Germany, E-mail: (r.vehmas@elettronica.de). *(Corresponding author: Nadav Neuberger.)*

I. INTRODUCTION

Phased array radar systems are nowadays ubiquitous in a large number of applications requiring reliable and continuous sensing of the environment. Recent new applications include fields such as human vital sign detection and tracking [1], [2], autonomous driving [3], [4], and space surveillance [5], [6]. The detection and localization of targets of interest are the key functionalities of the radar system in each of these applications. In estimating the target position, direction-of-arrival (DOA) estimation plays a crucial role. Emerging systems, such as the German Experimental Space Surveillance and Tracking Radar (GESTRA), whose purpose is to detect and track space debris [6], [7], consist of a large number of antenna elements to provide sensitive target detection and accurate DOA estimation.

However, when the number of elements is very large, data storage and real-time processing using element-level data become very demanding due to the high data dimension. The problem is especially severe for modern multiple-input multiple-output radar systems, which can consist of thousands of elements [8], [9]. This difficulty can be circumvented by transforming the full dimension element space (ESP) data into a reduced dimension beamspace (RDBS) via a linear transformation. Designing this transformation is of great practical importance because it directly affects the detection sensitivity and DOA estimation accuracy of the system.

Several beamspace transformation design methods have been considered in the literature. The most straightforward way is to cover a spatial sector of interest with steered sum beams of the receive array [10]. This can be interpreted as using a submatrix of the discrete Fourier transform as the beamspace transformation. Maximizing the average signal-to-noise ratio (SNR) inside a spatial sector of interest leads to a solution, where the transformation matrix is constructed using the eigenvectors of the signal correlation matrix [11], [12]. While this so-called discrete spheroidal sequence (DSS) method provides optimal detection performance, it does not guarantee optimal DOA estimation accuracy. On the other hand, the design method presented in [13] aims to provide exactly that the transformation is designed by requiring that it preserves the ESP Cramér–Rao bound (CRB) for 1-D DOA estimation at the true target locations.

The transformation design problem has also been considered in the context of nonlinear high-resolution estimation methods such as MUSIC [14] and ESPRIT [15]. The authors of [16]–[18] consider the beamspace implementation of these algorithms. More recently, beamspace MUSIC implementations have been used in through-the-wall radar imaging [19] and automotive radar applications [20]. The design criterion for the transformation remains quite subjective in these references, since it is hard to formulate optimality for biased estimators [21].

In many applications, achieving optimal estimation accuracy is not the only important criterion; interference suppression also plays a key role. The authors of [22]–[25]

consider designing the transformation so that a compromise between in-sector estimation accuracy and out-of-sector interference suppression can be achieved. As a drawback, many of these methods rely on suboptimal numerical optimization solutions to calculate the transformation matrix.

This article proposes two significant contributions related to the beamspace transformation design. The first is an extension to [13], which focuses on an optimal beamspace transformation. We propose a novel parameter-controlled RDBS to obtain a compromise between detection and DOA estimation performance when the RDBS dimension is insufficient to achieve optimality. Our method differs from [13] in two additional ways. We extend the optimal CRB approach to 2-D DOA and amplitude estimation. The inclusion of amplitude estimation is directly translated to detection performance. We also use a spatial target probability distribution to focus the performance on specific areas when *a priori* information about the targets is available.

The second contribution deals with the analysis of the RDBS performance. Usually, this evaluation is made by simulating each combination of RDBS dimension and spatial area size. A simple and clear view of potential performance is, therefore, not easy to atain. We introduce a new method to easily evaluate the possible performance for a given array, as a function of the resource ratio—the ratio between the RDBS dimension and spatial area coverage. Similar methods, to the knowledge of the authors, do not exist.

These contributions provide the radar system designer with valuable tools for the RDBS transformation matrix construction. They allow us to achieve optimal performance or an acceptable performance tradeoff for a specific use case. In practice, the available hardware and computational resources (e.g., number of Rx channels, time consumption, and data storage) dictate the RDBS dimension.

We have presented the outline of the proposed design method and preliminary results in a previous conference publication [26]. We do not consider interference suppression or multiple target scenarios in this article. Nevertheless, our method can be used together with interference suppression (such as [22]) and nonlinear high-resolution estimation methods. However, we note that in these cases, optimal performance is not necessarily preserved.

We start by introducing the theoretical background of the beamspace target detection and DOA estimation problems in Section II. We also formulate the required properties of the optimal beamspace transformation as the basis of our method. Section III presents our novel parameter-controlled method for dimension reduction. We then describe our new generalized transformation design tool in Section IV-B. Section V presents numerical simulation examples and discusses practical design issues highlighting the benefits of our design method. Finally, Section VI concludes this article.

II. THEORETICAL BACKGROUND

In this section, we define the underlying signal model of the RDBS and the related detection and estimation performances. Additionally, we discuss the beamspace target detection and DOA estimation problems. In the following text, we use lower- and uppercase boldface letters to denote vectors and matrices, respectively.

A. Signal Model

Let us consider a planar spatially symmetric 2-D phased array radar systems with N antenna elements. We limit our analysis to a time snapshot (i.e., single pulse) case with a single point target without interference. The jth antenna element response can be modeled as

$$y_j = a(\alpha, \phi)e^{ik\boldsymbol{r}_j^T\boldsymbol{u}} + n_j \tag{1}$$

$\forall j = 1, \ldots, N$. The two-way antenna element gain and the target reflectivity affect the deterministic complex amplitude $a(\alpha, \phi) = \alpha e^{i\phi}$ with positive $\alpha \in \mathbb{R}$ and $\phi \in [0, 2\pi)$. The directional cosine (DOA) vector $\boldsymbol{u} = [u\ v]^T \in \{\boldsymbol{u'} \in \mathbb{R}^2 | \ \|\boldsymbol{u'}\| \leq 1\}$ (called $\boldsymbol{u}$-space from here on), k is the wavenumber, and $\boldsymbol{r}_j = [x_j\ y_j]^T$ is the position vector of the jth element. The noise sample n_j originates from a complex zero mean white Gaussian process with variance σ^2. Rewriting the array response (1) in vector form yields the $N \times 1$ vector

$$\boldsymbol{y} = \boldsymbol{m}(\boldsymbol{\vartheta}) + \boldsymbol{n} \tag{2}$$

where $\boldsymbol{m}(\boldsymbol{\vartheta}) = a(\alpha, \phi)\boldsymbol{d}(\boldsymbol{u})$ with the target parameter vector $\boldsymbol{\vartheta} = [\alpha\ \phi\ u\ v]^T$. Since the noise is assumed to be independent and identically distributed across the elements, $\boldsymbol{n} \in \mathbb{C}^N$ with covariance $\boldsymbol{Q} = E\{\boldsymbol{n}\boldsymbol{n}^H\} = \sigma^2\boldsymbol{I}_N$, where $E\{\cdot\}$ stands for the statistical expectation and $(\cdot)^H$ for the Hermitian conjugate. The array steering vector $\boldsymbol{d} \in \mathbb{C}^N$ representing the phase delays between the elements is

$$\boldsymbol{d}(\boldsymbol{u}) = \begin{bmatrix} e^{ik\boldsymbol{r}_1^T\boldsymbol{u}} & e^{ik\boldsymbol{r}_2^T\boldsymbol{u}} & \ldots & e^{ik\boldsymbol{r}_N^T\boldsymbol{u}} \end{bmatrix}^T. \tag{3}$$

In the remainder of this article, we will focus on optimal ways to lower the dimensionality of the data received by the array. This is achieved by transforming the element-level data into an RDBS using a linear transformation matrix $\boldsymbol{B}$. Mathematically, this is expressed by

$$\boldsymbol{z} = \boldsymbol{B}^H\boldsymbol{y} = \boldsymbol{B}^H\boldsymbol{m}(\boldsymbol{\vartheta}) + \boldsymbol{B}^H\boldsymbol{n} = \tilde{\boldsymbol{m}}(\boldsymbol{\vartheta}) + \tilde{\boldsymbol{n}} \tag{4}$$

where $\boldsymbol{B} = [\boldsymbol{b}_1\ \ldots\ \boldsymbol{b}_M] \in \mathbb{C}^{N\times M}$ and $M \leq N$. The covariance of the transformed RDBS noise is $\boldsymbol{R} = E\{\tilde{\boldsymbol{n}}\tilde{\boldsymbol{n}}^H\} = E\{\boldsymbol{B}^H\boldsymbol{n}(\boldsymbol{B}^H\boldsymbol{n})^H\} = \sigma^2\boldsymbol{B}^H\boldsymbol{B}$. From here on, we use the term *beamformer* when referring to the beamspace transformation matrix $\boldsymbol{B}$.

In the considered radar application, we aim to detect a target and estimate its parameters. The objective is to detect the presence of a target with as low SNR as possible (i.e., high detection sensitivity) and estimate the parameters $\boldsymbol{\vartheta}$ (containing both amplitude and DOA) as accurately as possible (in terms of estimation variance). As we will show in the next section, the amplitude estimation accuracy essentially quantifies the detection performance. We now turn to study the effect of the beamformer on these aspects.

B. Target Detection and Parameter Estimation

In this article, we use the maximum likelihood (ML) estimator. It is asymptotically (as $N \to \infty$) unbiased with minimum variance [27]. These profound properties allow us to design a data dimension reduction method preserving performance optimality.

Other nonlinear estimation methods, such as the Capon method [28], [29] or MUSIC [14], can also be used for DOA estimation. These methods can provide increased performance when multiple targets are present due to their improved resolution and missing sidelobes. However, these advantages come at a cost. They require a good estimate for the signal covariance matrix and perform poorly for correlated targets. Additionally, the fact that these estimators are biased further complicates the issue.

The ML estimator is obtained by maximizing the likelihood function

$$L_B(\boldsymbol{\vartheta}; \boldsymbol{z}) = \frac{\exp\left[-(\boldsymbol{z} - \tilde{\boldsymbol{m}}(\boldsymbol{\vartheta}))^H \boldsymbol{R}^{-1} (\boldsymbol{z} - \tilde{\boldsymbol{m}}(\boldsymbol{\vartheta}))\right]}{\pi^M |\boldsymbol{R}|} \tag{5}$$

where $|\cdot|$ denotes the determinant of a matrix. This is equivalent with the known matched filter (MF) solution (see [30] and [31]) using the weight vector

$$\tilde{\boldsymbol{w}}(\boldsymbol{u}) = \frac{\boldsymbol{R}^{-1}\tilde{\boldsymbol{d}}(\boldsymbol{u})}{\sqrt{\tilde{\boldsymbol{d}}^H(\boldsymbol{u})\boldsymbol{R}^{-1}\tilde{\boldsymbol{d}}(\boldsymbol{u})}} \tag{6}$$

where $\tilde{\boldsymbol{d}}(\boldsymbol{\vartheta}) = \boldsymbol{B}^H \boldsymbol{d}(\boldsymbol{\vartheta})$. Thus, the ML estimate for $\boldsymbol{u}$ is obtained as

$$\boldsymbol{u}_{\mathsf{ML}} = \arg\max_{\boldsymbol{u}'} |\tilde{\boldsymbol{w}}^H(\boldsymbol{u}')\boldsymbol{z}|^2. \tag{7}$$

The solution of (7) can be obtained, e.g., by a numerical 2D grid search over the u-space. The weight vector depends only on u because the amplitude term a is obtained in closed form as a least squares solution (see [31]).

To declare a detection, the well-known Neyman–Pearson likelihood ratio test [27] is usually performed. It maximizes the probability of detection P_{D} for a given false alarm probability P_{FA} and a corresponding detection threshold T. The presence of a target is declared if $|\tilde{\boldsymbol{w}}^H(\boldsymbol{u})\boldsymbol{z}|^2 > T$.

C. Estimation Accuracy Analysis

A theoretical lower bound for the variance of any unbiased estimator is dictated by the CRB. We, therefore, analyze the estimation accuracy of the proposed beamformer by observing and comparing the corresponding CRB values. The CRB is the inverse of the Fisher information matrix $\boldsymbol{J}$, which is defined as the negative expectation of the Hessian of the log-likelihood function $\ln(L_B)$. For the RDBS data, we have

$$\boldsymbol{J}_B(\boldsymbol{\vartheta}) = -E\left\{\frac{\partial^2}{\partial\boldsymbol{\vartheta}\partial\boldsymbol{\vartheta}^T}\ln(L_B(\boldsymbol{\vartheta}; \boldsymbol{z}))\right\}. \tag{8}$$

Using the signal model (4) and noting that the beamformer $\boldsymbol{B}$ is independent of $\boldsymbol{\vartheta}$, the RDBS Fisher information is (see [10] and [32])

$$\begin{aligned}\boldsymbol{J}_B(\boldsymbol{\vartheta}) &= 2\Re\left\{\tilde{\boldsymbol{m}}_{\boldsymbol{\vartheta}}^H(\boldsymbol{\vartheta})\boldsymbol{R}^{-1}\tilde{\boldsymbol{m}}_{\boldsymbol{\vartheta}}(\boldsymbol{\vartheta})\right\} \\ &= \frac{2}{\sigma^2}\Re\left\{\boldsymbol{m}_{\boldsymbol{\vartheta}}^H(\boldsymbol{\vartheta})\boldsymbol{P}_{\boldsymbol{B}}\boldsymbol{m}_{\boldsymbol{\vartheta}}(\boldsymbol{\vartheta})\right\}\end{aligned} \tag{9}$$

where $\Re\{\cdot\}$ denotes the real part operator,

$$\begin{aligned}\boldsymbol{m}_{\boldsymbol{\vartheta}}(\boldsymbol{\vartheta}) &= \begin{bmatrix}\boldsymbol{m}_\alpha(\boldsymbol{\vartheta}) & \boldsymbol{m}_\phi(\boldsymbol{\vartheta}) & \boldsymbol{m}_u(\boldsymbol{\vartheta}) & \boldsymbol{m}_v(\boldsymbol{\vartheta})\end{bmatrix} \\ &\triangleq \begin{bmatrix}\frac{\partial \boldsymbol{m}(\boldsymbol{\vartheta})}{\partial\alpha} & \frac{\partial \boldsymbol{m}(\boldsymbol{\vartheta})}{\partial\phi} & \frac{\partial \boldsymbol{m}(\boldsymbol{\vartheta})}{\partial u} & \frac{\partial \boldsymbol{m}(\boldsymbol{\vartheta})}{\partial v}\end{bmatrix} \\ &= e^{i\phi}\begin{bmatrix}\boldsymbol{d}(\boldsymbol{u}) & i\alpha\boldsymbol{d}(\boldsymbol{u}) & i\alpha k\boldsymbol{x}\odot\boldsymbol{d}(\boldsymbol{u}) & i\alpha k\boldsymbol{y}\odot\boldsymbol{d}(\boldsymbol{u})\end{bmatrix}\end{aligned} \tag{10}$$

is the Jacobian of the target signal model $\boldsymbol{m}(\boldsymbol{\vartheta})$, and $\boldsymbol{P}_{\boldsymbol{B}} = \boldsymbol{B}(\boldsymbol{B}^H\boldsymbol{B})^{-1}\boldsymbol{B}^H$. In (10), $\boldsymbol{x}$ and $\boldsymbol{y}$ denote vectors containing the x and y positions of the array elements (Cartesian coordinates in the plane of the array) and $\odot$ denotes the Hadamard product. Similarly to (9), the ESP Fisher matrix can easily be calculated using $\boldsymbol{Q}$ instead of $\boldsymbol{R}$, which yields

$$\boldsymbol{J}_E(\boldsymbol{\vartheta}) = \frac{2}{\sigma^2}\Re\left\{\boldsymbol{m}_{\boldsymbol{\vartheta}}^H(\boldsymbol{\vartheta})\boldsymbol{m}_{\boldsymbol{\vartheta}}(\boldsymbol{\vartheta})\right\}. \tag{11}$$

The matrix $\boldsymbol{P}_{\boldsymbol{B}}$ has the form of a projection operator. When applied to an arbitrary N-dimensional vector, it projects the vector onto the range $\boldsymbol{B}$ of $\boldsymbol{B}$ (i.e., the subspace spanned by the columns of $\boldsymbol{B}$). Thus, we can make an important observation from (9). If the column vectors $\boldsymbol{m}_\gamma = \partial\boldsymbol{m}/\partial\gamma$ ($\gamma \in \{\alpha, \phi, u, v\}$) are not contained in $\boldsymbol{B}$, the diagonal elements of $\boldsymbol{J}_B$ are smaller than the corresponding elements in $\boldsymbol{J}_E$. This means that the dimension reduction leads to a loss of information, which, in turn, leads to increased values for the CRB matrix elements. Another important observation concerns the element of $\boldsymbol{J}_B$ related to estimating α. We have

$$\begin{aligned}\boldsymbol{J}_{B,\alpha\alpha}(\boldsymbol{\vartheta}) &= \frac{2}{\sigma^2}\Re\left\{\boldsymbol{m}_\alpha^H(\boldsymbol{\vartheta})\boldsymbol{P}_{\boldsymbol{B}}\boldsymbol{m}_\alpha(\boldsymbol{\vartheta})\right\} \\ &= \frac{2}{\sigma^2}\boldsymbol{d}^H(\boldsymbol{u})\boldsymbol{P}_{\boldsymbol{B}}\boldsymbol{d}(\boldsymbol{u}).\end{aligned} \tag{12}$$

This quantity is directly related to the estimated SNR (more precisely the SNR loss caused by the beamformer), which is the key factor determining detection performance. The optimum beamspace SNR of the MF is

$$\chi_B(\boldsymbol{\vartheta}) = |\tilde{\boldsymbol{w}}^H(\boldsymbol{u})\tilde{\boldsymbol{m}}(\boldsymbol{\vartheta})|^2 = \frac{1}{\sigma^2}\boldsymbol{m}^H(\boldsymbol{\vartheta})\boldsymbol{P}_{\boldsymbol{B}}\boldsymbol{m}(\boldsymbol{\vartheta}). \tag{13}$$

Thus, $\boldsymbol{J}_B$ contains the necessary information about both the detection and DOA estimation performance losses caused by the beamformer.

D. Optimal Beamformer

The properties of the $N \times M$ beamformer matrix $\boldsymbol{B}$, that achieves ESP detection and DOA estimation performance within a spatial sector of interest $\mathcal{U}$ in $\boldsymbol{u}$-space are described next.

Let $\boldsymbol{CRB}_E(\boldsymbol{\vartheta})$ and $\boldsymbol{CRB}_B(\boldsymbol{\vartheta})$ denote the ESP and RDBS CRB matrices, respectively. We use the term *design DOAs* to define a discrete set of DOAs $\boldsymbol{u}_i$ that cover the area

$\mathcal{U}$ ($\boldsymbol{u}_i \in \mathcal{U}\ \forall i = 1, \ldots, L$). The design DOAs are points (possible target locations) in which we require $\boldsymbol{CRB}_E$ to be preserved after applying the beamformer.

REMARK The elements of $\boldsymbol{CRB}_E(\boldsymbol{\vartheta})$ represent a lower bound for the estimation variance of any unbiased estimator for the unknown parameters in $\boldsymbol{\vartheta}$. Thus, the term "optimal" means equality of $\boldsymbol{CRB}_B$ with $\boldsymbol{CRB}_E$.

We can now formulate the relationship between the RDBS and ESP. We then deduce the needed properties of the transformation matrix.

THEOREM 1 Let $\boldsymbol{\Psi} = \{\boldsymbol{\vartheta}_1, \ldots, \boldsymbol{\vartheta}_L\}$ be a subdomain of the entire parameter space, restricted to the L design DOAs in $\mathcal{U}$. Furthermore, we define $\boldsymbol{B}$ as the range of the $N \times M$ matrix $\boldsymbol{B}$. Then, if the property

$$\boldsymbol{m}_\gamma(\boldsymbol{\vartheta}) \in \boldsymbol{B} \quad \forall \gamma \in \{\alpha, \phi, u, v\} \quad \forall \boldsymbol{\vartheta} \in \boldsymbol{\Psi} \tag{14}$$

is fulfilled, the beamformer $\boldsymbol{B}$ achieves optimal (ESP) performance.

PROOF From (14), we get $\boldsymbol{P_B m}_\gamma(\boldsymbol{\vartheta}) = \boldsymbol{m}_\gamma(\boldsymbol{\vartheta})$. It directly follows that

$$\frac{2}{\sigma^2}\Re\left\{\boldsymbol{m}_\gamma^H(\boldsymbol{\vartheta})\boldsymbol{P_B m}_{\gamma\prime}(\boldsymbol{\vartheta})\right\} = \frac{2}{\sigma^2}\Re\left\{\boldsymbol{m}_\gamma^H(\boldsymbol{\vartheta})\boldsymbol{m}_{\gamma\prime}(\boldsymbol{\vartheta})\right\}. \tag{15}$$

Therefore, using the result (15) above with (9)–(11), we get $\forall \boldsymbol{\vartheta} \in \boldsymbol{\Psi}$ the desired equalities

$$\boldsymbol{J}_B(\boldsymbol{\vartheta}) = \boldsymbol{J}_E(\boldsymbol{\vartheta}) \tag{16}$$

$$\boldsymbol{CRB}_B(\boldsymbol{\vartheta}) = \boldsymbol{CRB}_E(\boldsymbol{\vartheta}) \tag{17}$$

and

$$\chi_B(\boldsymbol{\vartheta}) = \chi_E(\boldsymbol{\vartheta}) \tag{18}$$

where $\chi_E(\boldsymbol{\vartheta})$ is the ESP SNR. ■

The simplest way to satisfy (14) is to construct $\boldsymbol{B}$ by using the vectors $\boldsymbol{m}_\gamma(\boldsymbol{\vartheta})$ as its columns. Since we have L design DOAs and four vectors $\boldsymbol{m}_\gamma$ corresponding to each of them, $M = 4L$.

The value of L depends on two factors: the size of $\mathcal{U}$ and the spacing between the design DOAs. The beamwidth of the array dictates a reasonable upper limit for the spacing (since two vectors $\boldsymbol{m}$ spaced a beamwidth apart are linearly independent). To get a nearly uniform performance inside $\mathcal{U}$, the spacing should be a fraction of the beamwidth (for further discussion, see Section V-D).

REMARK Let

$$\hat{\boldsymbol{m}}_{\boldsymbol{\vartheta}}(\boldsymbol{\vartheta}_i) = \left[\hat{\boldsymbol{m}}_\alpha(\boldsymbol{\vartheta}_i) \quad \hat{\boldsymbol{m}}_\phi(\boldsymbol{\vartheta}_i) \quad \hat{\boldsymbol{m}}_u(\boldsymbol{\vartheta}_i) \quad \hat{\boldsymbol{m}}_v(\boldsymbol{\vartheta}_i)\right] \tag{19}$$

denote the $N \times 4$ matrix consisting of unit vectors $\hat{\boldsymbol{m}}_\gamma(\boldsymbol{\vartheta}_i) = \boldsymbol{m}_\gamma(\boldsymbol{\vartheta}_i)/\|\boldsymbol{m}_\gamma(\boldsymbol{\vartheta}_i)\|$. Following (10) yields

$$\hat{\boldsymbol{m}}_\alpha(\boldsymbol{\vartheta}_i) = e^{i\phi}\frac{\boldsymbol{d}(\boldsymbol{u}_i)}{\|\boldsymbol{d}(\boldsymbol{u}_i)\|}$$

$$\hat{\boldsymbol{m}}_\phi(\boldsymbol{\vartheta}_i) = ie^{i\phi}\frac{\boldsymbol{d}(\boldsymbol{u}_i)}{\|\boldsymbol{d}(\boldsymbol{u}_i)\|}$$

$$\hat{\boldsymbol{m}}_u(\boldsymbol{\vartheta}_i) = ie^{i\phi}\frac{\boldsymbol{x} \odot \boldsymbol{d}(\boldsymbol{u}_i)}{\|\boldsymbol{x} \odot \boldsymbol{d}(\boldsymbol{u}_i)\|}$$

$$\hat{\boldsymbol{m}}_v(\boldsymbol{\vartheta}_i) = ie^{i\phi}\frac{\boldsymbol{y} \odot \boldsymbol{d}(\boldsymbol{u}_i)}{\|\boldsymbol{y} \odot \boldsymbol{d}(\boldsymbol{u}_i)\|}. \tag{20}$$

We have $\hat{\boldsymbol{m}}_\alpha(\boldsymbol{\vartheta}_i) = \varepsilon\hat{\boldsymbol{m}}_\phi(\boldsymbol{\vartheta}_i)$, where ε is a complex constant. Moreover, the unit vectors do not depend on the amplitude (α) of the signal. Thus, we can replace $\hat{\boldsymbol{m}}_{\boldsymbol{\vartheta}}(\boldsymbol{\vartheta}_i) = \hat{\boldsymbol{m}}_{\boldsymbol{\vartheta}}([1\ 0\ u_i\ v_i])$ with $\hat{\boldsymbol{m}}_{\boldsymbol{\vartheta}}(\boldsymbol{u}_i)$.

Consequently, we have only three linearly independent vectors corresponding to each design DOA $\boldsymbol{u}_i$. Since $\hat{\boldsymbol{m}}_\phi = i\hat{\boldsymbol{m}}_\alpha$ is omitted, we can construct $\boldsymbol{B}$ with $M = 3L$ columns. When $3L \geq N$, we note that $\boldsymbol{B} = \boldsymbol{I}_N$ is the optimal beamformer.

III. PARAMETER-CONTROLLED BEAMFORMER

In practice, having $3L$ channels is too high for most systems. We aim to reduce RDBS dimension as much as possible while maintaining desired performance. A well-known mathematical method called the singular value decomposition (SVD) can be used to construct the optimal transformation matrix with a lower dimension than $3L$. The ability to optimally reduce dimensions using this process depends on the rank of the decomposed matrix.

Our objective is to find the matrix satisfying (14), minimize its rank appropriately—considering the practical limitations and performance criteria—and then perform the SVD. The beamformer $\boldsymbol{B}$ will then be constructed from the SVD. We define

$$\hat{\boldsymbol{\Omega}} = [\hat{\boldsymbol{m}}_\alpha(\boldsymbol{u}_1) \quad \hat{\boldsymbol{m}}_u(\boldsymbol{u}_1) \quad \hat{\boldsymbol{m}}_v(\boldsymbol{u}_1) \quad \ldots \quad \hat{\boldsymbol{m}}_\alpha(\boldsymbol{u}_L) \quad \hat{\boldsymbol{m}}_u(\boldsymbol{u}_L) \quad \hat{\boldsymbol{m}}_v(\boldsymbol{u}_L)] \tag{21}$$

as a collection of unit vectors in the form of an $N \times 3L$ matrix that covers all the design DOAs and satisfies (14). Taking the SVD of (21) is analogous with the method in [13]. We have extended it to accommodate the full 4-D CRB matrix (including complex target amplitude and 2-D DOA) instead of the 1-D DOA CRB. Next, we will propose two novel techniques to lower the rank R_Ω of $\hat{\boldsymbol{\Omega}}$ prior to performing the SVD.

We also note that by spanning the unit vectors $\hat{\boldsymbol{m}}_\gamma(\boldsymbol{u})$ $\forall \gamma \in \{\alpha, \phi, u, v\}$, we will equally weight them in the SVD. Since they are a function of $\boldsymbol{u}$ only, the beamformer construction will not depend on the amplitude, i.e., the SNR (see remark after Theorem 1).

A. Rank Reduction

A first possible step to decrease R_Ω is by accommodating an *a priori* target distribution $p(\boldsymbol{u})$ over $\mathcal{U}$. We define the $N \times 3L$ matrix

$$\hat{\boldsymbol{\Omega}}^p = \left[\sqrt{p(\boldsymbol{u}_1)}\hat{\boldsymbol{m}}_\alpha(\boldsymbol{u}_1) \quad \sqrt{p(\boldsymbol{u}_1)}\hat{\boldsymbol{m}}_u(\boldsymbol{u}_1) \quad \ldots \quad \sqrt{p(\boldsymbol{u}_L)}\hat{\boldsymbol{m}}_u(\boldsymbol{u}_L) \quad \sqrt{p(\boldsymbol{u}_L)}\hat{\boldsymbol{m}}_v(\boldsymbol{u}_L)\right]. \tag{22}$$

The spatial target probability distribution p in (22) weights the unit vectors so that targets with high (low) probability will have high (low) impact on the SVD. If p is close to zero in certain parts of $\mathcal{U}$, the number of singular values that are close to zero increases (because the number of linearly

independent columns in $\hat{\boldsymbol{\Omega}}^p$ decreases) and R_Ω will decrease to $R_\Omega^p = \text{rank}(\hat{\boldsymbol{\Omega}}^p)$.

Since the left singular vectors of a matrix $\boldsymbol{A}$ are the eigenvectors of $\boldsymbol{A}\boldsymbol{A}^H$, we can write the $N \times N$ matrix

$$\hat{\boldsymbol{\Omega}}^p \hat{\boldsymbol{\Omega}}^{p^H} = \sum_{i=1}^{L} [\hat{\boldsymbol{m}}_\alpha(\boldsymbol{u}_i)\hat{\boldsymbol{m}}_\alpha^H(\boldsymbol{u}_i) + \hat{\boldsymbol{m}}_u(\boldsymbol{u}_i)\hat{\boldsymbol{m}}_u^H(\boldsymbol{u}_i) + \hat{\boldsymbol{m}}_v(\boldsymbol{u}_i)\hat{\boldsymbol{m}}_v^H(\boldsymbol{u}_i)]p(\boldsymbol{u}_i) \quad (23)$$

and perform the eigenvalue decomposition (EVD) instead of the SVD.

REMARK If $\boldsymbol{J}_E(\boldsymbol{\vartheta})$ is diagonal, the elements of the diagonal $\boldsymbol{CRB}_B(\boldsymbol{\vartheta})$ matrix will be

$$\boldsymbol{CRB}_{B,\gamma\gamma}(\boldsymbol{\vartheta}) = \left[\frac{2}{\sigma^2}\Re\left\{\boldsymbol{m}_\gamma^H(\boldsymbol{\vartheta})\boldsymbol{B}\boldsymbol{B}^H\boldsymbol{m}_\gamma(\boldsymbol{\vartheta})\right\}\right]^{-1} \quad (24)$$

$\forall\gamma \in \{\alpha, \phi, u, v\}$ and $\forall\boldsymbol{\vartheta} \in \boldsymbol{\Psi}$. The diagonal elements depend only on a single parameter (no mixed parameter derivatives). The Fisher information matrix $\boldsymbol{J}_E$ is diagonal if the array is spatially symmetric, i.e., fulfilling that $\forall j, l = 1, \ldots, N$ and $\boldsymbol{r}_j = [x_j\, y_j]$, there exists $\boldsymbol{r}_l = 2\boldsymbol{r}_p - \boldsymbol{r}_j$ for $l \neq j$ and array center point $\boldsymbol{r}_p$.

To further reduce the rank of (23), we introduce a control parameter β. Let $\boldsymbol{J}_E(\boldsymbol{\vartheta})$ be diagonal $\forall\boldsymbol{\vartheta} \in \boldsymbol{\Psi}$ and

$$\hat{\boldsymbol{\Omega}}_\beta^p \hat{\boldsymbol{\Omega}}_\beta^{p^H} \triangleq \sum_{i=1}^{L} [(1-\beta)\hat{\boldsymbol{m}}_\alpha(\boldsymbol{u}_i)\hat{\boldsymbol{m}}_\alpha^H(\boldsymbol{u}_i) + \beta(\hat{\boldsymbol{m}}_u(\boldsymbol{u}_i)\hat{\boldsymbol{m}}_u^H(\boldsymbol{u}_i) + \hat{\boldsymbol{m}}_v(\boldsymbol{u}_i)\hat{\boldsymbol{m}}_v^H(\boldsymbol{u}_i))]p(\boldsymbol{u}_i) \quad (25)$$

with $0 \leq \beta \leq 1$. We can see that β allows us to obtain a tradeoff between DOA estimation and detection performance. More specifically, increasing β increases the impact of the vectors that relates to DOA estimation ($\hat{\boldsymbol{m}}_u, \hat{\boldsymbol{m}}_v$) on the account of amplitude estimation ($\hat{\boldsymbol{m}}_\alpha$), and *vice versa*.

We justify our claim about the performance tradeoff by observing two distinct cases, $\beta = 0, 1$. As seen from (25), the first ($\beta = 0$) will discard any knowledge of $\hat{\boldsymbol{m}}_u$ and $\hat{\boldsymbol{m}}_v$ from the following EVD. Therefore, assuming that $\boldsymbol{B}$ contains all the eigenvectors of (25) that correspond to nonzero eigenvalues, we get $\boldsymbol{m}_\alpha^H\boldsymbol{B}\boldsymbol{B}^H\boldsymbol{m}_\alpha = \boldsymbol{m}_\alpha^H\boldsymbol{m}_\alpha$, while $\boldsymbol{m}_u^H\boldsymbol{B}\boldsymbol{B}^H\boldsymbol{m}_u \leq \boldsymbol{m}_u^H\boldsymbol{m}_u$ (and correspondingly for $\boldsymbol{m}_v$). Hence, the CRB for the amplitude estimation is at minimum, while the DOA estimation CRB is degraded. The same logic applies for $\beta = 1$ with the opposite outcome. For increasing values of β, the performance for detection (amplitude estimation) degrades, while the DOA estimation performance improves.

We point out that the analytical formulation presented above relies on the assumption of uncorrelated noise (diagonal $\boldsymbol{Q}$). It is not possible to obtain a similarly easy analytical solution for a more general covariance matrix representing correlated noise or interference.

B. Beamformer Construction

Finally, we execute the EVD as $\hat{\boldsymbol{\Omega}}_\beta^p \hat{\boldsymbol{\Omega}}_\beta^{p^H} = \tilde{\boldsymbol{U}}_\beta \boldsymbol{\Lambda} \tilde{\boldsymbol{U}}_\beta^H$ with a decreasing order of eigenvalues and take the M first columns of $\tilde{\boldsymbol{U}}_\beta$ as $\boldsymbol{B}$. We denote $R_\Omega^\beta = \text{rank}(\hat{\boldsymbol{\Omega}}_\beta^p)$. The number of nonzero eigenvalues determines whether M yields optimal ($M \geq R_\Omega^\beta$) or suboptimal ($M < R_\Omega^\beta$) performance.

In Fig. 1, we illustrate the differences between the DOA estimation ($\beta = 1$) and detection ($\beta = 0$) beamformers. The power of the beams $\boldsymbol{b}_i^H\boldsymbol{d}(\boldsymbol{u})$ is shown for a square area $\mathcal{U}$ of size $4 \times \text{BW}_a$, where BW_a is the square approximation of the area confined inside the 3-dB beamwidth BW (0.1×0.1 in (u, v)-coordinates) of the array sum beam power pattern.

We can regard β as a way to reduce R_Ω^β according to predetermined performance criteria. We also note that the numerical rank calculation is not always straightforward, as it involves setting heuristic thresholds (outside the scope of this article). Hence, it is not possible to accurately determine the needed number of channels M that ensures optimality (ESP performance). Moreover, since the set of unit vectors $\{\boldsymbol{m}_\alpha(\boldsymbol{u}_i), \boldsymbol{m}_u(\boldsymbol{u}_i), \boldsymbol{m}_v(\boldsymbol{u}_i) : \; i \in \{1, \ldots, 3L\}\}$ might not be completely linearly independent, it is not possible to analytically determine the exact impact of β on the performance.

Therefore, in order to illustrate the impact of β and estimate the needed number of channels to achieve the desired performance (suboptimal or optimal), the next section presents a new design tool to aid in the beamformer construction.

IV. BEAMFORMER PERFORMANCE ANALYSIS

So far, we have presented the theory behind the proposed Rx beamformer. As (25) suggests, a set of values $\mathcal{J} = \{\beta, M, \mathcal{U}\}$ must be carefully determined to construct the beamformer. For that purpose, we propose a simple design tool, which takes into account the practical scenario of interest and a set of chosen performance metrics. It enables the user to design their beamformer by exploiting quantitative measures of potential performance.

In this article, we use target detection and DOA estimation metrics assuming a single target inside the field of view without any clutter or interference (space surveillance is a good example of such a scenario). Other metrics, such as target resolution or interference suppression, are not considered. We also assume a flat SNR level inside the $\mathcal{U}$ area.

A. Performance Metrics

First, we need to quantify the effect of the dimension reduction on target detection and DOA estimation. To this end, we analyze the following metrics.

1) *Detection:* The first metric evaluates the expectation of detection performance over $\mathcal{U}$ using $p(\boldsymbol{u})$. The expectation is normalized by the equivalent ESP performance. This can be formulated by

$$\kappa_m = E\{\text{SNR}_L\} \quad (26)$$

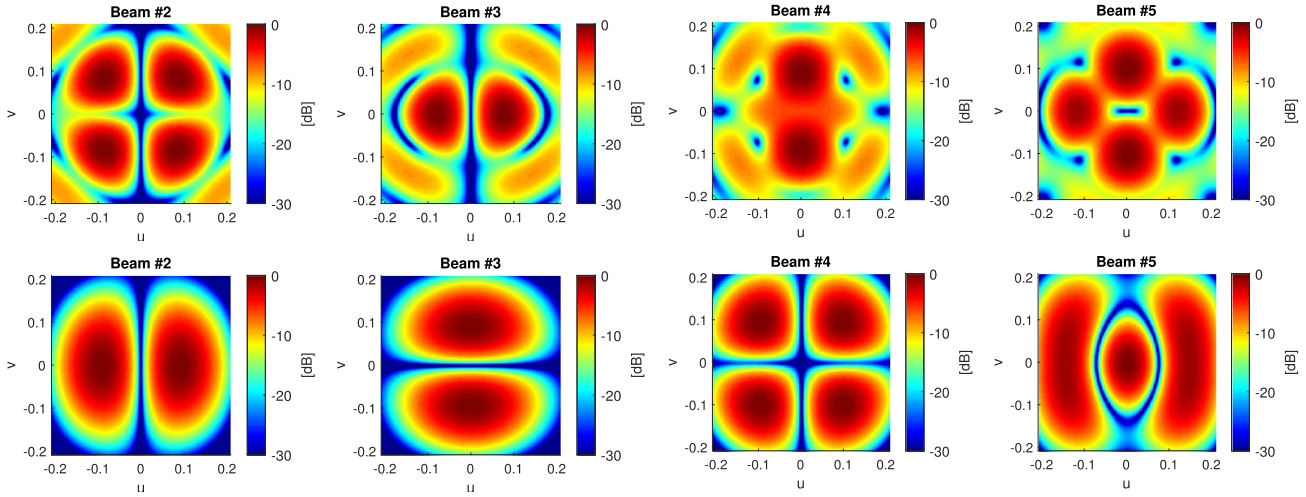

Fig. 1. Power patterns of selected four beams $\boldsymbol{b}_i$ for the optimal DOA estimation ($\beta = 1$, top row) and detection ($\beta = 0$, bottom row) beamformers. The similarity to monopulse difference beams is visible in detection beams 2 and 3. Beam 1 (omitted) resembles a conventional sum beam in both cases.

where

$$\mathrm{SNR}_L = \frac{\boldsymbol{d}^H(\boldsymbol{u})\boldsymbol{P}_{\boldsymbol{B}}\boldsymbol{d}(\boldsymbol{u})}{\boldsymbol{d}^H(\boldsymbol{u})\boldsymbol{d}(\boldsymbol{u})}. \tag{27}$$

The quantity κ_m can be interpreted in two equivalent ways. First, it is the average ratio between the ESP and RDBS CRBs for the amplitude (α) estimation. Second, it is the average SNR loss (relative to ESP sum beam) of the RDBS MF output inside $\mathcal{U}$. Thus, it quantifies the detection performance of the beamformer since the probability of detection P_{D} is inversely proportional to the SNR loss.

The distribution of (27) within $\mathcal{U}$ is also a crucial factor, often disregarded. It is possible to have a high value for κ_m with areas where the SNR loss is very high and no target can be detected (i.e., "blind zones"). Clearly, such a scenario is undesirable. We, therefore, calculate the relative standard deviation (STD) of (27) (normalized by κ_m) as

$$\kappa_{\mathrm{std}} = \frac{\sqrt{E\left\{\mathrm{SNR}_L{}^2\right\} - E\left\{\mathrm{SNR}_L\right\}^2}}{E\left\{\mathrm{SNR}_L\right\}} \tag{28}$$

to quantify the variation within $\mathcal{U}$.

2) *DOA Estimation:* To evaluate the DOA estimation performance, we consider the theoretical accuracy limit dictated by the CRB. Specifically, we analyze the accuracy by taking the square root of the determinant of the lower right 2×2 submatrix of the 4×4 $\boldsymbol{CRB}$ matrix, containing the terms related to estimating $\boldsymbol{u}$. We denote the RDBS and ESP determinants as

$$D_B = \sqrt{|\boldsymbol{CRB}_B(\boldsymbol{u})|} \text{ and } D_E = \sqrt{|\boldsymbol{CRB}_E(\boldsymbol{u})|}. \tag{29}$$

These can be interpreted as the 2-D ellipsoid areas defined by the CRB matrices in (u, v)-coordinates. The ratio

$$\eta_m = \frac{E\left\{D_B\right\}}{E\left\{D_E\right\}} \tag{30}$$

is used to compare the beamformer to the optimal ESP case. It represents the average CRB metric loss in DOA estimation.

It would be desirable to achieve a constant estimation performance independent of $\boldsymbol{u}$. To quantify the variation inside $\mathcal{U}$, we calculate the relative STD as

$$\eta_{\mathrm{std}} = \frac{\sqrt{E\left\{D_B{}^2\right\} - E\left\{D_B\right\}^2}}{E\left\{D_B\right\}}. \tag{31}$$

The chosen set of metrics is, therefore, $\mathcal{G} = \{\kappa_m, \kappa_{\mathrm{std}}, \eta_m, \eta_{\mathrm{std}}\}$.

B. Design Considerations

Equipped with the set of metrics $\mathcal{G}$, the user can specify acceptable thresholds for the metric values (performance tradeoff criteria) to meet their needs. Our design tool enables the user to analytically calculate the metrics in $\mathcal{G}$ for any (symmetrical) array, for a wide range of $\mathcal{U}$ area sizes, number of channels M, and β values. For any unbiased estimator, the consequently chosen set $\mathcal{J}$ leads to the best possible performance to be expected in terms of $\mathcal{G}$.

We define the term *resource ratio* as

$$\zeta = \frac{M}{\rho} \tag{32}$$

where ρ is the area size covered by $\mathcal{U}$ in units of $[\mathrm{BW}_a]$. Now, we claim that the chosen metrics will depend on M and ρ only through ζ. This is due to the fact that ρ determines R_Ω^β and, thus, the required number of channels to achieve a desired performance. The claim would be exact if we replaced ρ with R_Ω^β in (32). However, because the exact rank is difficult to determine numerically, we choose to stay with ρ and treat our claim as a good approximation.

The value of R_Ω^β also depends on the chosen value for β. It increases faster (with respect to ρ) for the DOA estimation beamformer than for the detection beamformer. For $\beta = 1$,

we have two linearly independent vectors for each design DOA, whereas for $\beta = 0$, we only have one. To avoid any problems, we always choose the geometrical boundary so that R_{Ω}^{β} monotonically increases with increasing ρ. The exact shape (e.g., square or rectangle) has a minor effect because R_{Ω}^{β} changes differently depending on how the area is increased.

To determine the optimal $\mathcal{J}$, we propose evaluating the metrics in $\mathcal{G}$ as a function of ζ and β. In practice, the user has a limited set of interesting values for ζ (mostly restricted by hardware capabilities) for which the metrics can be calculated as a function of β. This enables the user to choose $\mathcal{J}$ to meet the desired metric thresholds for $\mathcal{G}$. We demonstrate this process in more detail in the next section.

V. NUMERICAL RESULTS

In this section, we present numerical simulations to support the statements and theory presented in this article. The simulative study also serves as a walk-through on constructing and using the proposed design tool. The last part demonstrates the use of the design tool in a space surveillance scenario, inspired by the novel GESTRA system (see [6] and [7]).

A. Simulation Setup

We chose the following parameters for our simulations.

1) A circular phased array was used with $N = 256$ isotropic antenna elements spaced half-wavelength apart.
2) A set of rectangular $\mathcal{U}$ area sizes in units of [BW$_a$] was chosen. The v dimension was fixed to $2 \times$ BW, while the u dimension linearly increased from $2 \times$ BW to $5 \times$ BW with a step size of 0.5, resulting in $4 \leq \rho \leq 10$ [BW$_a$].
3) Targets (design DOAs) of equal SNR were placed inside $\mathcal{U}$ with a spacing of $1/10 \times$ BW to calculate the values in (26)–(31) and $\mathcal{G}$.
4) A set of channel numbers M was chosen as $5 \leq M \leq 15$.
5) A set of discrete values for β was chosen between $0 \leq \beta \leq 1$ with a step size of 0.1.
6) A uniform target probability density function $p(\boldsymbol{u})$ was used.

We emphasize the generality of the following plots used in our design tool. They are valid for every (symmetric) array, regardless of the number of elements, exact geometry, or SNR level. As previously stated, the geometrical shape of $\mathcal{U}$ (e.g., square or rectangle) has a minor effect. Nevertheless, for a nonuniform target probability distribution p, the following plots will have to be recalculated.

B. Validation and Analysis

In Fig. 2, we demonstrate the DOA estimation performance D_B inside $\mathcal{U}$ for $M = 10$ and $\rho = 10$ (i.e., $\zeta = 1$) and $\beta = 0, 1$. The plots illustrate the variation of D_B (captured by η_{std}) inside $\mathcal{U}$, which is different for each beamformer configuration.

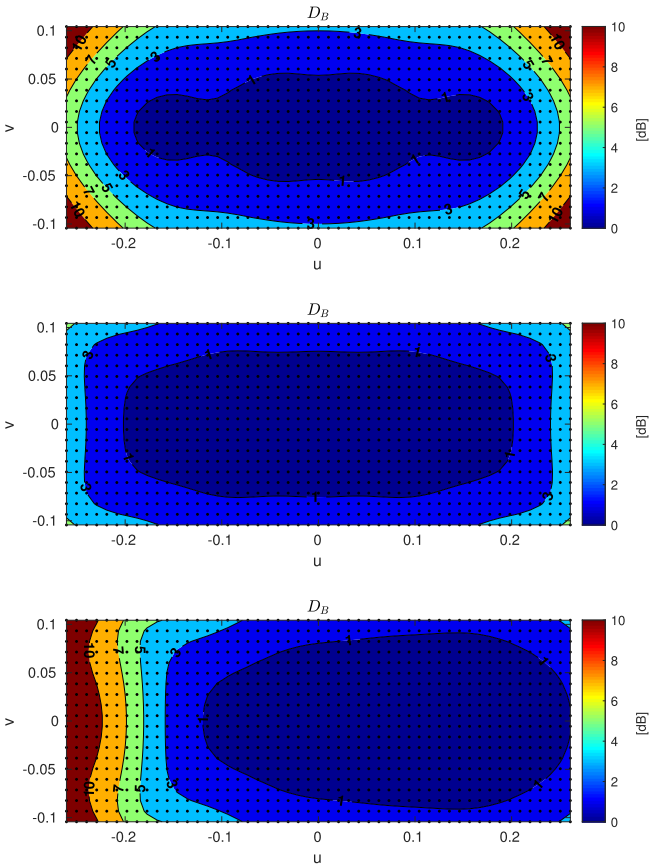

Fig. 2. Distribution of the theoretical estimation performance D_B over the spatial sector of interest $\mathcal{U}$ for the detection ($\beta = 0$, top) and DOA estimation ($\beta = 1$, middle and bottom) beamformers. The bottom result is obtained using a Gaussian target distribution p centered at (0.15, 0), while the other results are obtained with a uniform target distribution.

The black dots in the figure represent the target locations used to calculate D_B (i.e., the design DOAs). The uppermost plot shows the result for $\beta = 0$ (detection), while the center plot is for $\beta = 1$ (DOA estimation). In both cases, the CRB loss is monotonically increasing toward the edge of $\mathcal{U}$. For $\beta = 1$, the increase is smaller, resulting in a more uniform performance and a smaller value for η_{std}. In both of the aforementioned cases, the target probability distribution p is uniform.

The lowermost plot shows the result for $\beta = 1$ using a Gaussian distribution p with a half-power beamwidth of 0.15 centered at (0.15, 0). The target is assumed to be in the vicinity based on *a priori* information. The value of D_B in the vicinity of the expected target position is about 2 dB lower than in the case of a uniform distribution. The target probability p can also be used to account for a nonuniform transmit power pattern. Alternatively, p can utilize the information provided by a target detection from a previous pulse to obtain better performance for the current pulse.

Next, we provide a numerical validation of the previous claim that the resource ratio ζ is the key factor determining

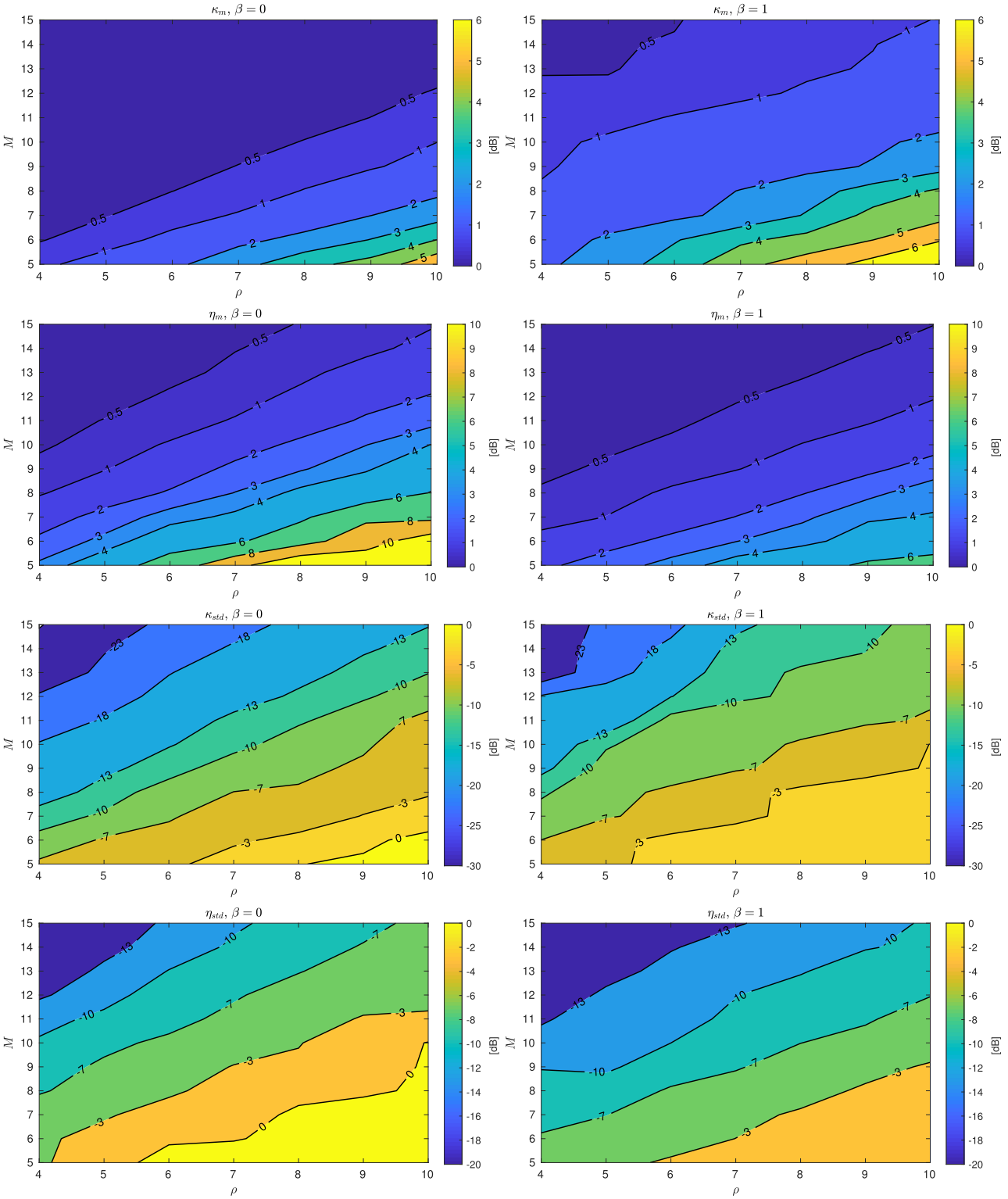

Fig. 3. Theoretical detection and estimation performance comparison between the beamformers. Each of the metrics is approximately constant along lines of constant resource ratio M/ρ.

the performance. In Fig. 3, each of the metrics in $\mathcal{G}$ is plotted as a function of M and ρ. The plots correspond to the two choices of $\beta = 0, 1$ as indicated in the plot titles. We clearly see that equal performance is achieved along straight lines with constant ζ to a high degree of accuracy (although we only present limited choices of β, we verified the results for all values of β). Equivalently, for an increasing ρ, the number of channels M required to maintain the same metric value increases.

The significance of the weighting factor β is also illustrated in the results of Fig. 3. The choice of $\beta = 1$ achieves the best performance for the DOA metrics $\{\eta_m, \eta_{\text{std}}\}$ for any

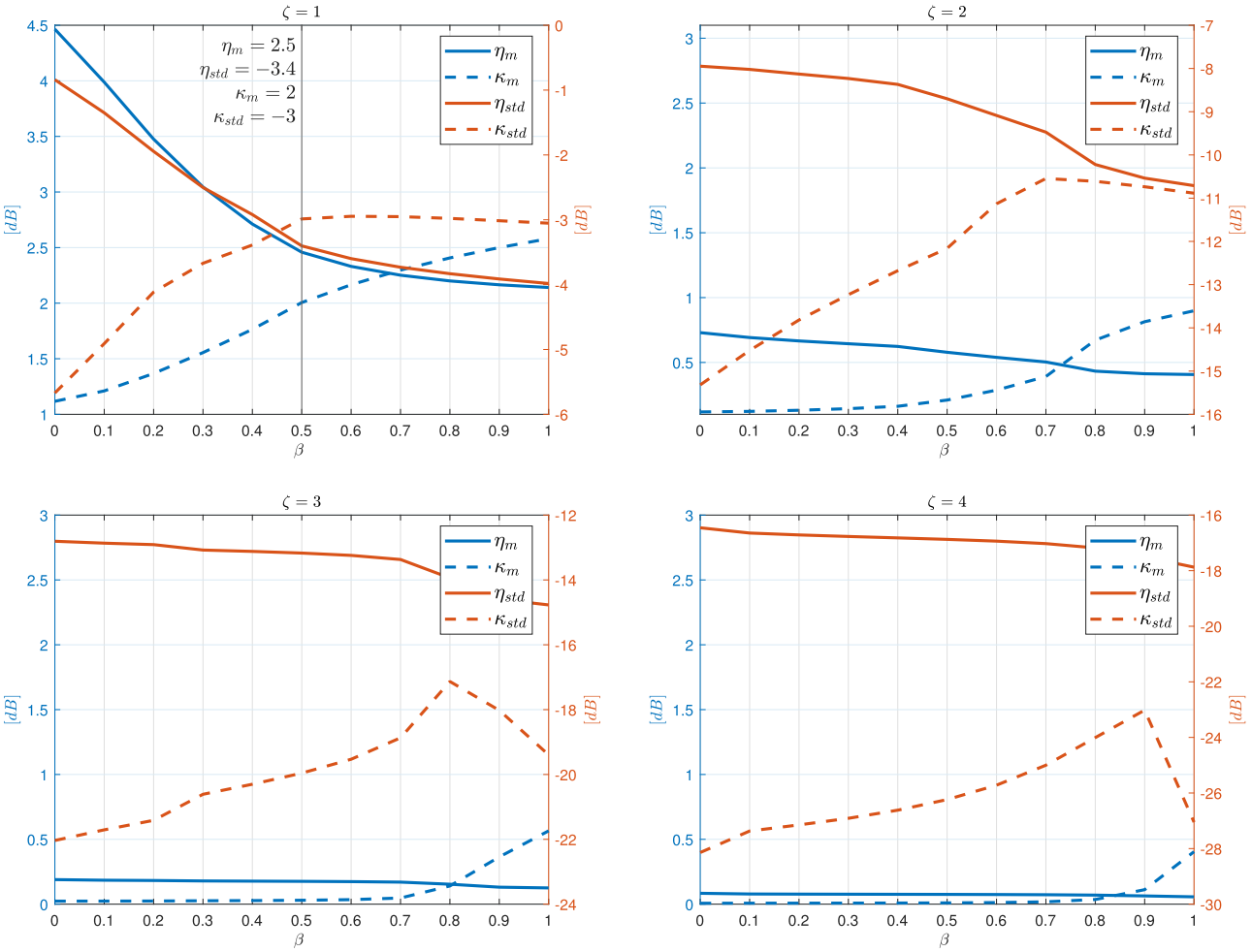

Fig. 4. Theoretical detection and estimation performance as a function of the control parameter β. These generalized plots enable the user to choose a desired performance tradeoff for a given number of channels and area size (resource ratio ζ). The scale on the left side and the corresponding blue lines represent the mean metrics, while the scale on the right side and the corresponding red lines depict the STD metrics.

combination of M and ρ. The same applies for $\beta = 0$ and the SNR metrics $\{\kappa_m, \kappa_{\text{std}}\}$. For $\beta \in [0, 1]$, the metrics in $\mathcal{G}$ are affected differently and bounded by their values for the cases of $\beta = \{0, 1\}$. As a general observation, we see that $M \ll N$ channels are sufficient to achieve ESP performance, even for large area sizes of $\mathcal{U}$ (assuming the metrics concerning the STD are at acceptable levels).

C. Design Tool Construction

Next, we implement the proposed design tool described in Section IV-B. Possible resource availability cases were categorized into $\zeta = \{1, 2, 3, 4\}$, representing low to high resource ratios, respectively. For each case, the metrics $\mathcal{G}$ were evaluated as a function of β. To illustrate the significance relative to previous methods, we note that $\beta = 0$ corresponds to a 2-D version of the DSS method [12] and $\beta = 1$ to a 2-D version of [13].

A new set of figures was created by mapping the data from Fig. 3 in the following manner. For each metric and β, the data along a constant contour line were mapped into a figure corresponding to the line's slope, determined by ζ. Therefore, we have four plots corresponding to the chosen values of ζ in Fig. 4.

We conclude that for a low resource ratio $\zeta = 1$, the detection ($\beta = 0$) and DOA estimation ($\beta = 1$) beamformers perform differently, exhibiting a substantial gap between the metric values. Moreover, the effect of β becomes clearly visible. As β increases from 0 to 1, the DOA metrics are monotonically improving: η_m drops from 4.5 dB down to almost 2 dB, and η_{std} from -1 to -4 dB. However, the detection metrics are monotonically degrading: κ_m increases from 1 to 2.5 dB, and κ_{std} from -6 to -3 dB. This illustrates the previously mentioned tradeoff, which can be controlled by β.

Several more observations can be made. As the resource ratio increases, all metrics improve. The case of $\zeta = 4$ can be considered as a practical performance limit (for any array), as it almost converges to ESP values. In addition, the impact of β reduces, and the metrics $\{\eta_m, \kappa_m\}$ approximately reach a constant response as a function of β. When the channel number increases (while ρ remains fixed), the number of omitted eigenvectors corresponding to nonzero eigenvalues decreases, making β redundant.

For validation purposes, additional configurations were simulated, comprising of different number of elements, array, and $\mathcal{U}$ area geometries. The obtained results very accurately matched the ones presented above, serving as an additional verification that the key factor in the calculations is the resource ratio ζ.

D. Beamformer Construction Procedure

We now summarize the required steps of the proposed design tool of Section IV-B to construct the beamformer. First, the set of values $\mathcal{J}$ is determined as follows.

1) Calculate the resource ratio ζ from (32), taking into account the available number of channels and required $\mathcal{U}$ area.
2) Set the needed thresholds for the metrics in $\mathcal{G}$ (i.e., quantify an acceptable performance tradeoff).
3) Refer to the matching plot for ζ in Fig. 4. Choose the corresponding β value where the defined metric thresholds are met. However, if such a value for β does not exist, the only possible solution is to consider a higher resource ratio.

We denote the outcome of these steps as $\mathcal{J}_0 = \{\beta_0, M_0, \mathcal{U}_0\}$. Second, we outline how to construct the beamformer as described in Section III (we note that $p(\boldsymbol{u}) = 1$ in this scenario).

1) Define a set of design DOAs $\boldsymbol{u}_i$ covering the spatial area of interest $\mathcal{U}_0$. The spacing should be sufficiently small to ensure homogeneous coverage. The exact spacing should be verified empirically based on the metrics in $\mathcal{G}$. In our simulations, a spacing of BW/10 produced satisfactory results: decreasing the spacing further showed little to no change in the results.
2) Calculate (25) with the chosen set $\mathcal{J}_0$ and perform the eigendecomposition with descending eigenvalues. Take the first M_0 eigenvectors as $\boldsymbol{B}$.

E. Use-Case Demonstration

To demonstrate a practical application of the proposed design tool, we consider the following scenario. The system is operated in a search mode, where the objective is to detect the target and estimate its DOA within a rectangular shaped area $\mathcal{U}_0$ of 2×4 [BW], meaning that $\rho_0 = 8$. The available number of channels, dictated by the available hardware resources, is set to $M_0 = 8$.

Using the same simulation setup, $L = 1020$ and $R_\Omega = \{107, 119\}$ for $\beta = \{0, 1\}$, respectively. Clearly, constructing an optimal beamformer satisfying Theorem 1 is impossible, since $M \ll \{3L, R_\Omega\}$. Thus, we turn to a suboptimal solution using the procedure described in Section III-A. First, we calculate $\zeta_0 = M_0/\rho_0 = 8/8 = 1$. Second, we set the thresholds for the metrics in $\mathcal{G}$ with common-practice values (in [dB]): $\eta_m \leq 3$, $\kappa_m \leq 3$, $\eta_{\text{std}} \leq -3$, and $\kappa_{\text{std}} \leq -3$. Finally, we use the upper-left plot in Fig. 4 to find the matching β value: By intersecting a vertical line (representing a fixed value of β) with the metric curves, we see that $\beta = 0.5$ meets these criteria.

Our design tool makes it very easy to understand the performance limitations. All possible values for the metrics in $\mathcal{G}$ for a given ζ are clearly visible in Fig. 4. The benefit of using our design method is highlighted: We are able to meet the desired performance (with limited resources) by tuning β. Otherwise, this would only be possible by increasing the number of channels, which may not be feasible due to practical limitations.

F. Monte Carlo Simulations

The preceding numerical results represent the theoretical values (e.g., CRB) obtained using the various analytical formulations given throughout this article. In this section, we validate that these ideal theoretical results are close to practically achievable performance with a realistic system, where a numerical estimator for $\boldsymbol{\vartheta}$ is used.

To achieve this, we carried out empirical numerical simulations based on the ML estimator with the underlying signal model, as described in (4). To avoid any undesirable numerical errors, we used a sequential brute force optimization on a grid with decreasing spacing to locate the ML maximum according to (7). For each combination of the setup parameters and design DOAs, the simulation was repeated $N_{\text{MC}} = 100$ times with a different white Gaussian noise realization to allow sufficient statistical accuracy.

An example of the obtained empirical results is depicted in Fig. 5 for $\beta = 0$. We first calculated the empirical covariance of the DOA estimations over the MC iterations, denoted as $\boldsymbol{COV}_B(\boldsymbol{u})$. Similarly to (29) and (30), we calculated $D_C = \sqrt{|\boldsymbol{COV}_B(\boldsymbol{u})|}$ and the mismatch as $\tau_m = E\{D_C\}/E\{D_B\}$. This result is shown on the left-hand side of Fig. 5.

Since the ML estimator is *asymptotically* unbiased, the right-hand side Fig. 5 aims to validate the bias of the MC estimations (should ideally tend to zero). The mean bias over $\mathcal{U}$ was calculated and normalized by ${D_B}^{1/4}$ for proper scaling (denoted as ν_b).

For high resource ratios, we have a very low covariance mismatch (below 0.5 dB) and bias level (below -18 dB), implying an excellent agreement with theoretical calculations. However, for low resource ratios and inadequate target SNR, we observed a considerable mismatch.

Often overlooked, this so-called *ambiguity* problem may have an undesirable effect: When the number of channels is not high enough to uniformly cover the entire area $\mathcal{U}$ (low resource ratio $\zeta < 1$), multiple equally high peaks emerge in the ML function. These peaks can be explained by the normalization factor in (6), which is (apart from a constant factor) the square root of the SNR loss in (27). A low resource ratio causes the SNR loss to vary significantly inside $\mathcal{U}$, which, in turn, causes amplification of the sidelobes of the target response.

If this phenomenon is not taken into account during the detection stage, the estimation algorithm can choose the sidelobes peak as the maximum, leading to unreliable detection and estimation results. This behavior causes the empirical estimation to have an increased covariance and

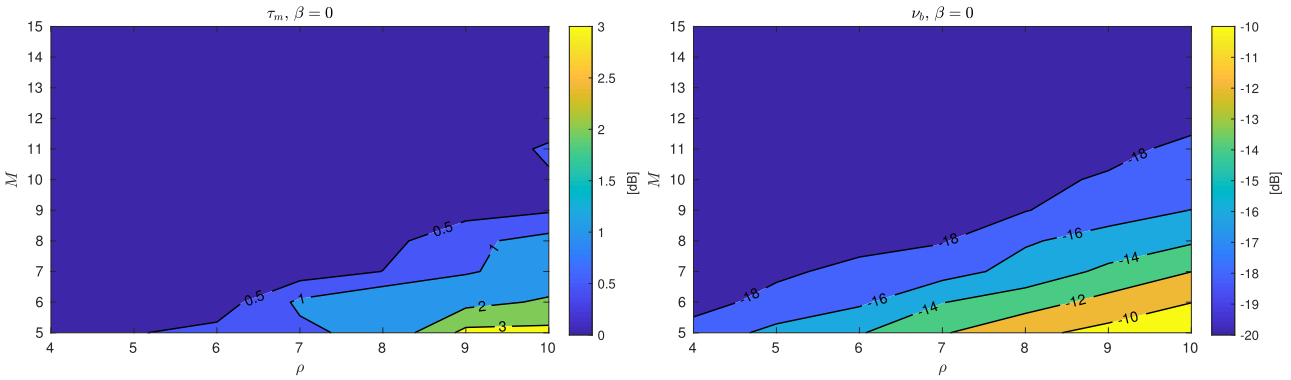

Fig. 5. Comparison between theoretical and empirical results. On the left-hand side, the ratio between the empirical covariance and the CRB is shown. The discrepancy for low resource ratios in the bottom right corner can be explained by the estimation bias caused by the ambiguous estimation results, which is depicted on the right-hand side.

a significant bias. This is depicted in the results shown in Fig. 5. For low resource ratios (bottom right corners), the bias ν_b increases from -20 to -10 dB relative to the mean (plot on the right), and the estimated covariance mismatch τ_m reaches up to 3 dB relative to the theoretical one (plot on the left).

These values suggest that we are unable to obtain performance comparable to the CRB for very low resource ratios with the chosen target SNR of -9 dB (at element level) used in our MC simulations. We point out this potentially unwanted outcome, but further investigation of this ambiguity problem is outside the scope of this article.

VI. CONCLUSION

In this article, we have presented an elaborated formulation to the phased array Rx data dimension reduction transformation process. First, we proposed a method to construct a beamformer simultaneously achieving optimal target detection and 2-D DOA estimation performance. When the number of channels is too low to achieve optimality, we introduced a new parameter-controlled design method to obtain a performance tradeoff between target detection and DOA estimation.

Thereafter, we generalized our findings into a novel design tool, which allows the user to evaluate potential beamformer performance for a given practical use case and then construct one to meet desired criteria. Finally, we performed numerical studies to provide validation, a walk-through demonstration of the design process, and an overview of important practical considerations.

The analysis presented in this article can be further extended in several ways. One example is to consider the optimal transformation design for nonlinear high-resolution estimation methods (e.g., MUSIC, Capon, or ESPRIT). Another is to investigate new performance metrics, such as target resolution and interference suppression in the design criteria.

Analyzing the impact of additional factors on the design tool may also be considered. These include more complicated noise and interference models, channel calibration errors, nonsymmetrical arrays, nonsymmetrical coverage areas, and nonuniform target probability densities.

REFERENCES

[1] M. Mercuri, I. R. Lorato, Y.-H. Liu, F. Wieringa, C. Van Hoof, and T. Torfs
Vital-sign monitoring and spatial tracking of multiple people using a contactless radar-based sensor
Nature Electron., vol. 2, no. 6, pp. 252–262, 2019.

[2] S. Wang, S. Kueppers, H. Cetinkaya, and R. Herschel
3D localization and vital sign detection of human subjects with a 120 GHz MIMO radar
In *Proc. 20th Int. Radar Symp.*, Jun. 2019, pp. 1–6.

[3] S. M. Patole, M. Torlak, D. Wang, and M. Ali
Automotive radars: A review of signal processing techniques
IEEE Signal Process. Mag., vol. 34, no. 2, pp. 22–35, Mar. 2017.

[4] S. Brisken, F. Ruf, and F. Höhne
Recent evolution of automotive imaging radar and its information content
IET Radar, Sonar Navigat., vol. 12, no. 10, pp. 1078–1081, Sep. 2018.

[5] M. Th, J. Eglizeaud, and J. Bouchard
GRAVES: The new french system for space surveillance
In *Proc. 4th Eur. Conf. Space Debris*, Apr. 2005, pp. 61–66.

[6] H. Wilden *et al.*
"GESTRA—A phased-array based surveillance and tracking radar for space situational awareness
In *Proc. IEEE Int. Symp. Phased Array Syst. Technol.*, Oct. 2016, pp. 1–5.

[7] H. Wilden *et al.*
"GESTRA—Recent progress, mode design and signal processing
In *Proc. IEEE Int. Symp. Phased Array Syst. Technol.*, Oct. 2019, pp. 1–8.

[8] T. Lv, F. Tan, H. Gao, and S. Yang
A beamspace approach for 2-D localization of incoherently distributed sources in massive MIMO systems
Signal Process., vol. 121, pp. 30–45, 2016.

[9] Z. Zheng, W. Wang, H. Meng, H. C. So, and H. Zhang
Efficient beamspace-based algorithm for two-dimensional DOA estimation of incoherently distributed sources in massive MIMO systems
IEEE Trans. Veh. Technol., vol. 67, no. 12, pp. 11 776–11789, Dec. 2018.

[10] H. L. Van Trees
Optimum Array Processing: Part IV of Detection, Estimation, and Modulation Theory. Hoboken, NJ, USA: Wiley, 2004.

[11] P. Forster and G. Vezzosi
Application of spheroidal sequences to array processing
In *Proc. IEEE Int. Conf. Acoust., Speech, Signal Process.*, 1987, vol. 12, pp. 2268–2271.

[12] B. Van Veen and B. Williams
Structured covariance matrices and dimensionality reduction in array processing
In *Proc. 4th Annu. ASSP Workshop Spectr. Estimation Model.*, Aug. 1988, pp. 168–171.

[13] S. Anderson
On optimal dimension reduction for sensor array signal processing
Signal Process., vol. 30, no. 2, pp. 245–256, 1993.

[14] R. Schmidt
Multiple emitter location and signal parameter estimation
IEEE Trans. Antennas Propag., vol. 34, no. 3, pp. 276–280, Mar. 1986.

[15] R. Roy and T. Kailath
ESPRIT-estimation of signal parameters via rotational invariance techniques
IEEE Trans. Acoust., Speech, Signal Process., vol. 37, no. 7, pp. 984–995, Jul. 1989.

[16] H. B. Lee and M. S. Wengrovitz
Resolution threshold of beamspace MUSIC for two closely spaced emitters
IEEE Trans. Acoust., Speech, Signal Process., vol. 38, no. 9, pp. 1545–1559, Sep. 1990.

[17] M. D. Zoltowski, S. D. Silverstein, and C. P. Mathews
Beamspace root-MUSIC for minimum redundancy linear arrays
IEEE Trans. Signal Process., vol. 41, no. 7, pp. 2502–2507, Jul. 1993.

[18] G. Xu, S. D. Silverstein, R. H. Roy, and T. Kailath
Beamspace ESPRIT
IEEE Trans. Signal Process., vol. 42, no. 2, pp. 349–356, Feb. 1994.

[19] Y. Yoon and M. G. Amin
High-resolution through-the-wall radar imaging using beamspace MUSIC
IEEE Trans. Antennas Propag., vol. 56, no. 6, pp. 1763–1774, Jun. 2008.

[20] Y. Li, C. Zhang, Y. Song, and Y. Huang
Enhanced beamspace MUSIC for cost-effective FMCW automotive radar
IET Radar, Sonar Navigat., vol. 14, no. 2, pp. 257–267, Feb. 2020.

[21] F. Li and H. Liu
Statistical analysis of beam-space estimation for direction-of-arrivals
IEEE Trans. Signal Process., vol. 42, no. 3, pp. 604–610, Mar. 1994.

[22] M. Li and Y. Lu
Dimension reduction for array processing with robust interference cancellation
IEEE Trans. Aerosp. Electron. Syst., vol. 42, no. 1, pp. 103–112, Jan. 2006.

[23] A. Hassanien, S. A. Elkader, A. B. Gershman, and K. M. Wong
Convex optimization based beam-space preprocessing with improved robustness against out-of-sector sources
IEEE Trans. Signal Process., vol. 54, no. 5, pp. 1587–1595, May 2006.

[24] A. Hassanien and S. A. Vorobyov
A robust adaptive dimension reduction technique with application to array processing
IEEE Signal Process. Lett., vol. 16, no. 1, pp. 22–25, Jan. 2009.

[25] M. Li, K. S. Ho, and G. Hayward
Beamspace transformation for data reduction using genetic algorithms
In *Proc. IEEE Int. Ultrasonics Symp.* Sep. 2009, pp. 702–705.

[26] N. Neuberger, R. Vehmas, and J. Ender
A parameter-controlled Rx beamspace transformation design method
In *Proc. IEEE Radar Conf.*, 2020, pp. 1–6.

[27] S. M. Kay
Fundamentals of Statistical Signal Processing. Englewood Cliffs, NJ, USA: Prentice-Hall, 1993.

[28] J. Capon
High-resolution frequency-wavenumber spectrum analysis
Proc. IEEE, vol. 57, no. 8, pp. 1408–1418, Aug. 1969.

[29] J. Li, P. Stoica, and Z. Wang
On robust capon beamforming and diagonal loading
IEEE Trans. Signal Process., vol. 51, no. 7, pp. 1702–1715, Jul. 2003.

[30] U. Nickel
Monopulse estimation with adaptive arrays
Proc. Inst. Elect. Eng. F—Radar Signal Process., vol. 140, no. 5, pp. 303–308, Oct. 1993.

[31] U. Nickel
Overview of generalized monopulse estimation
IEEE Aerosp. Electron. Syst. Mag., vol. 21, no. 6, pp. 27–56, Jun. 2006.

[32] P. Stoica and A. Nehorai
Performance study of conditional and unconditional direction-of-arrival estimation
IEEE Trans. Acoust., Speech, Signal Process., vol. 38, no. 10, pp. 1783–1795, Oct. 1990.

Nadav Neuberger (Member, IEEE) received the B.Sc. degree in electrical and computer engineering from Ben-Gurion University, Be'er Sheva, Israel, in 2012, and the M.Sc. degree in electrical and electronic engineering from Tel Aviv University, Tel Aviv, Israel, in 2017. He is currently working toward the Ph.D. degree in electrical engineering with Siegen University, Siegen, Germany.

After completing the B.Sc. degree, he worked as an Electrical Engineer in the private sector in large companies and small scale start-ups. Since 2018, he has been with the Fraunhofer Institute for High Frequency Physics and Radar Techniques FHR, Wachtberg, Germany. His major research areas were electromagnetics and human vital signs monitoring through radar. His current research interests include phased array radar signal processing in the space surveillance awareness scenario.

Risto Vehmas received the M.Sc. degree in theoretical physics from the University of Oulu, Oulu, Finland, in 2014, and the Ph.D. degree in computing and electrical engineering from the Tampere University of Technology, Tampere, Finland, in 2018.

From 2019 to 2020, he was with the Fraunhofer Institute for High Frequency Physics and Radar Techniques FHR, Wachtberg, Germany, where his research focused on signal processing algorithms for array-based radar systems. He is currently with Elettronica GmbH, Meckenheim, Germany, where he works as a System Analyst.

Joachim H. G. Ender was head of the Fraunhofer Institute for High Frequency Physics and Radar Techniques FHR in Wachtberg and holder of the Chair for High Frequency Sensors and Radar Techniques at the University of Siegen until July 2016. After receiving his diploma in mathematics/physics, he has been conducting research on various topics in radar science for more than forty years. He started his career in 1976 as a junior scientist, was appointed head of department in 1999, and finally took over the position of director of Fraunhofer FHR in 2003.

After his retirement, he is still active as Senior Scientist at FHR and as Senior Member and Professor at the Center for Sensor Systems (ZESS) of the University of Siegen. Prof. Dr.-Ing. Joachim Ender is author and co-author of numerous papers. Among others, he was awarded the “Group Technical Achievement Award - For contributions to Array Signal Processing and Multichannel Synthetic Aperture Radar” by EURASIP. In 2014, he was named an IEEE Fellow “for contributions to Multichannel Synthetic Aperture Radar and Radar Array Signal Processing”. He was one of the founding members of the "European Conference on Synthetic Aperture Radar" (EUSAR), which has been held every two years since 1996.